

Indigenous alkaliphiles as an effective tool for bioremediation of bauxite residue (red mud)



Ankita Naykodi^a, Kruthi Doriya^{b,*}, Bhaskar N. Thorat^c

^a Department of Biotechnology, Institute of Chemical Technology- IndianOil Odisha Campus, Bhubaneswar, 751013, Odisha, India

^b Department of Chemical Engineering, Institute of Chemical Technology-IndianOil Odisha Campus, Bhubaneswar, 751013, Odisha, India

^c Department of Chemical Engineering, Institute of Chemical Technology Mumbai, 400019, India

ARTICLE INFO

Keywords:

Alkaliphiles
Metal tolerance
Bauxite residue
Bioremediation
Neutralization

ABSTRACT

The microorganisms thriving in ageing Bauxite residue, or red mud, have captured scientific interest for their adaptability to extreme conditions. This study investigates extremophilic microbial communities present in Indian red mud for their potential to neutralize the residue and extracting metals. These communities thrive in the highly alkaline, sodic, and metal-rich conditions of this challenging environment. The research specifically highlights alkali-halophilic species and their ability to withstand pH fluctuations (7–11) and varying NaCl levels (0–3 M). Out of the 13 isolates analyzed, all preferred a pH range of 9–10 and tolerated NaCl up to 1.5–2 M. Notably, *Evansella cellosilytica* and *Halalkalibacterium halodurans*, showed superior tolerance index for Al³⁺ and Cr⁶⁺ at 2000 ppm, as well as Co²⁺ at 1000 ppm, followed by *Sutcliffiella cohnii*. However, the tolerance index for Cu²⁺, Te⁴⁺, and Hg²⁺ was relatively low for all tested strains. Additionally, *Alkalihalobacillus* sp. demonstrated remarkable tolerance to 10% red mud, facilitated by the production of mixed acids, neutralizing the pH within 24 h. The study proposes a potential mechanism for metal and red mud tolerance through genomic analysis using Rapid Annotation Subsystem Technology (RAST), revealing stress tolerance mechanisms, metal resistance genes, ion transporters, hydrolytic enzymes, siderophore production, and organic acid synthesis. Indigenous species like *E. cellosilytica*, *H. halodurans*, *S. cohnii*, and *Alkalihalobacillus* sp. emerge as promising candidates for red mud bioremediation, providing insights into sustainable strategies for red mud disposal.

1. Introduction

Metals and metalloids toxicity is significantly influenced by environmental and microbiological factors, including metal binding, precipitation, complexation, and ionic interactions. Moreover, the form in which metals and metalloids are present in the environment determines their toxicity. Gu (2016) highlights the importance of assessing the bioavailable form of metals and metalloids accurately when conducting toxicity assessments. Microbes possess diverse tolerance mechanisms, indicating broad detoxification strategies beyond metal-contaminated environments (Gadd et al., 1977). To address pollution concerns in metal extraction industries from hazardous waste, sustainable microbial technologies are crucial (Zhuang et al., 2015). Alkaliphilic species, such as *Alkaliphilus metallireducens*, are promising for metal-contaminated sites with alkaline environments (Roh et al., 2007). These microbes thrive in high pH conditions, providing a cleaner and more efficient approach to metal recycling (Sarethy et al., 2011). For instance,

A. metallireducens (QYMF) is a metal-reducing bacterium isolated from a leachate pond with pH 9.0–10.0 and sodium concentration of 440–12, 100 ppm. This bacterium can convert soluble iron and phosphate from the leachate into less toxic forms (Roh et al., 2007). Similarly, *Amphibacillus* sp. strain KSU isolated from a hypersaline soda lake was effective in chromium reduction under alkaline and high sodium concentrations (Ibrahim et al., 2011). Interestingly alkaliphilic species are also capable of converting alkaline environment into neutral one (Kulshreshtha et al., 2010). Therefore, these alkaliphilic species can be utilized for bioremediation and bacteria-assisted phytoremediation in metal-contaminated alkaline soils due to their high resistance and diverse detoxification mechanisms (González Henao and Ghneim-Herrera, 2021; Wilks et al., 2009).

The alumina industry struggles in managing alkaline and saline Bauxite residue also known as red mud, a byproduct with high disposal needs (Qaidi et al., 2022). On average, the production of one ton of alumina generates 1.5–2 tons of red mud, leading to substantial waste

* Corresponding author.

E-mail address: k.doriya@iocb.ictmumbai.edu.in (K. Doriya).

volume (Naykodi et al., 2023). This complex waste, rich in elements such as aluminum, iron, and titanium, is typically deposited in ponds, creating a global environmental challenge. The 2010 red mud dam failure at the Ajka alumina plant in Hungary highlighted the urgent need for improved red mud storage solutions (Anam et al., 2019). The toxicity of red mud due to high alkalinity and salinity is a major threat to air, water and land ecological systems (Ilkhani et al., 2024). Therefore, initial efforts have focused on mitigating red mud's toxicity and alkalinity to enable its reuse (Ujaczki et al., 2018). In industrial settings, inorganic leaching is commonly employed; however, researchers have explored bio-neutralization methods using both indigenous and non-indigenous acidophilic species (Panda et al., 2017). Additionally bioleaching with metal-tolerant microbes offers a sustainable alternative to bioremediate red mud (Tran et al., 2020). Fungal species such as *Aspergillus* and *Penicillium* have been promising in metal extraction from red mud, while *Acetobacter* and *Gluconobacter* also exhibit bioleaching potential (Abhilash and Schippers, 2021; Kiskira et al., 2021; Qu et al., 2015; Shah et al., 2022). However, scaling up bioleaching requires a deeper understanding of indigenous extremophile communities, as non-indigenous species often struggle to adapt. A hybrid bioleaching approach involving oxalic acid pretreatment followed by bioleaching was employed by Ilkhani et al. (2024) to recover rare earth elements (REE) from red mud. The authors also highlighted the importance of bio-organic acid produced by alkali-halo tolerant bacterial species in the leaching of REEs. Therefore, comprehensive studies on microbial communities within red mud are essential. Krishna et al. (2014) suggest that red mud serves as a unique model system characterized by alkaline, saline, sodic conditions, heavy metal contamination, and low organic carbon and nitrogen levels. This presents a valuable opportunity to explore biological interactions and survival mechanisms in such unique environments. Few studies have identified microbial species thriving within red mud. Agnew et al. (1995) first reported the presence of *Bacillus veddari*, followed by subsequent studies confirming the prevalence of *Bacillus* sp. in red mud by Nogueira et al. (2017) and Wu et al. (2019). Qu et al. (2019) observed the presence of *Acetobacter* sp. in two-decade-old red mud, demonstrating its potential for bioleaching applications. Researchers are also investigating the potential of non-enriched biomass for red mud bioremediation (Cozzolino et al., 2023). However, the large-scale application of this approach faces challenges due to its slow kinetics and low efficiency.

In India, Krishna et al. (2014) and then Dey and Paul (2021) discovered rich microbial communities within Indian red mud. These communities encompassed both culturable and non-culturable organisms, predominantly affiliated with the Firmicutes, Actinobacteria, and Proteobacteria phyla. However, to date, no studies have been reported on red mud detoxification/neutralization using native alkaliphilic strains. This has prompted the current investigation of discovering the extremophilic diversity within red mud (sourced from the NALCO Damanjodi plant in Odisha) with the potential of neutralization and metal removal capability. The primary objective was to evaluate the tolerance of alkali-halophilic species to various stress conditions, such as pH (7–11), NaCl (0–3 M) concentrations, exposure to metals including Al³⁺(100–2000 ppm), Cu²⁺(100–2000 ppm), Co²⁺(100–2000 ppm), Cr⁶⁺(100–2000 ppm), Te⁴⁺(100–1000 ppm), Hg²⁺(50–1000 ppm), and their resilience to red mud exposure (up to 10%). Previously, researchers have established selection criteria for microorganisms that are suitable for red mud bioremediation (Hamdy, 2001; Santini et al., 2015). Based on these criteria, isolated and identified alkali-halophilic strains exhibit tolerance to alkalinity and salinity, demonstrate non-pathogenicity, and produce organic acids and exopolysaccharides. Furthermore, their metal tolerance enhances their suitability for direct application in red mud neutralization and metal extraction studies.

Using the Rapid Annotation using Subsystem Technology (RAST) server, genome analysis of the isolates was conducted to identify genes associated with metal resistance, ion transporters, hydrolytic enzymes, and the synthesis of organic acids, exopolysaccharides, and

siderophores. The analysis confirmed the presence of various metal resistance genes, including aluminum, mercury, tellurite resistance protein and chromate reductase. Moreover, the identification of multiple efflux pumps, ABC transporters and a multidrug efflux system highlighted the additional tolerance mechanisms. Based on this information, the probable mechanism of metal tolerance in the isolated species was also elucidated, which is crucial for understanding their tolerance to multiple metals and red mud. Moreover, the study reveals potential for exopolysaccharide and organic acid production in these isolates. Together, these metabolic capabilities position the isolated alkali-halophilic species as promising candidates for red mud bioremediation.

To the best of our knowledge, this is the first study in which alkali-halophilic species have adjusted the pH of red mud to neutral or slightly acidic in less than 24 h. This study demonstrates that the challenges associated with the large-scale utilization of red mud can be overcome using native alkaliphiles.

2. Materials and methods

2.1. Sample Collection and preservation

Red mud samples were collected from the NALCO plant located in Damanjodi, Odisha. Two types of samples were obtained.

- Fresh red mud: Directly obtained from the plant, representing the material in its initial state.
- Aged red mud: Seven samples were collected from two locations within the storage pond, as detailed in Table 1.

The aged red mud samples were collected from different depths to capture substantially maximum microflora present within the storage area. For instance, surface and subsurface samples represent air-borne bacterial species. On the other hand, the deep layer (30–40 cm) and carbonate layers may have red mud-adapted species. Collected samples were preserved at a constant temperature of 4 °C in a refrigerator until the commencement of subsequent analyses. The low temperature was chosen to inhibit any potential chemical reactions or alterations in the samples during storage (Krishna et al., 2014).

2.2. Characterization of red mud samples

The following approach was used to characterize new red mud samples. Wet red mud was pulverized into a fine powder after being crushed and dried at 110 °C for 4–5 h (Qu et al., 2013). A homogeneous powder with a particle size of less than 63 µm was produced using a sieve shaker. A pH meter (Apera instruments pH 9500, China) was used to measure the pH. For pH analysis, solutions of various concentrations of red mud were prepared using distilled water and autoclaved at 121 °C for 15 min. The elemental analysis of red mud was carried out using X-ray fluorescence (Axios-MAX PANalytical, Japan) and Inductive coupled plasma-mass spectroscopy (PerkinElmer Avio 200 ICP OES model USA). The Fourier Transformed Infrared (FTIR) analysis was conducted using a FTIR spectrometer (JASCO FT-IR 4200, Japan) across the 400–4000 cm⁻¹ wavelength range. Subsequently, transmittance

Table 1
Sampling of red mud.

Location name	Sample names		
Red mud pond	Location 1	Surface	RPS1
		Subsurface	RPS1
		30–40 cm deep	RPD1
	Location 2	Surface CO3	RPCO
		Surface	RPS2
		Subsurface	RPS2
		30–40 cm deep	RPD2

versus wavenumber spectra were generated and plotted.

2.3. Enrichment and isolation of bacteria from red mud

Aged samples were subjected to enrichment by adding 1:10 diluted Horikoshi medium (Horikoshi 1999) and nutrient broth separately. Each sample, weighing 1 g, was mixed with 100 mL of both mediums and then incubated at 30 °C under static conditions. The isolation was carried out on the 4th, 9th, and 15th day of enrichment using nutrient agar and Horikoshi agar plates. All plates were incubated at 37 °C until visible growth occurred. A total of 15 isolates with distinct morphologies were obtained. Subsequently, mixed cultures were purified.

2.4. 16 S-rRNA sequencing and phylogenetic analysis

For 16 S-rRNA sequencing, DNA extraction was performed on all 15 isolates using the Quick-DNA™ Fungal/Bacterial Miniprep Kit from Zymo Research. The isolated DNA underwent electrophoresis on an agarose gel to assess its purity based on the 260/280 ratio. Additionally, Nanodrop was employed to determine the DNA concentration. Subsequently, PCR (Veriti™, Thermal cycler 96 well fast) was conducted on the isolated and purified DNA using 16 S rRNA-specific primers (27 F and 1492 R) with the following primer sequences:

27 F: GAGTTTGATCATGGCTCAG.

1492 R: TACGGTTACCTTGTACGACTT.

Following the 16 S-rRNA sequencing, phylogenetic analysis was performed using MegaX (Tamura et al., 2011) software. The PCR protocol involved a 25 µL reaction volume consisting of 10 pmol each of forward and reverse primers, 2.5 mM of MgCl₂, 200 µM of each of the four deoxyribonucleotide triphosphates (dNTPs), 0.5 U of Taq DNA polymerase, 1x concentration of PCR buffer (Invitrogen, Life Technologies, Brazil), and 50–100 ng of isolated bacterial genomic DNA.

The PCR process included an initial denaturation step at 95 °C for 5 min, followed by 39 cycles of denaturation for 30 s at 95 °C, annealing for 45 s, and elongation at 72 °C for 1 min. The final extension was carried out for 7 min at 72 °C. The resulting amplicons were analyzed on a 1.5% agarose gel using 0.5X tris-acetate-EDTA (TAE) buffer. Bi-directional DNA sequencing was performed on the PCR amplicons using the 27 F and 1492 R primers with the BDT v3.1 Cycle sequencing kit on ABI 3500Dx Genetic Analyzer.

2.5. Growth curve

In the growth curve experiment, the culture was initiated by introducing 1 mL of a culture with an initial optical density (OD) of 0.1(10⁷ CFU/ml) into 100 mL of St. Horikoshi broth with a pH of 10.3. Subsequently, it was incubated at a constant temperature of 37 °C with agitation at 150 rpm. Samples were collected at 4 h intervals, and the optical density at 600 nm was measured using a double beam UV-Visible spectrophotometer (Shimadzu UV1900i, Japan). In the case of isolate RPS1.2, 0.5 M NaCl was incorporated into the St. Horikoshi broth with a pH of 10.3.

(Note: Optical density OD~ 0.1 equal to 10⁷ CFU/ml for all bacterial cultures except RPS2.2, RPD1.2 and RPD2.1. For these 3 cultures, OD~ 0.1 is averagely equal to 10⁵–10⁶ CFU/ml)

2.6. Effect of pH on growth

To evaluate pH tolerance, 200 µL of a culture with an initial optical density (OD) of 0.1 was inoculated into 5 mL of Horikoshi broth. We then adjusted the pH of the broth to various levels within the range of 7–11 by using 4 M sodium hydroxide. After 24 h incubation at 37 °C with agitation at 150 rpm, optical density was measured at 600 nm using a UV-visible spectrophotometer (Ibrahim et al., 2019; Joshi et al., 2021). pH measurements were carried out on the culture supernatant, which was obtained post-centrifugation at 5000 rpm for 20 min.

2.7. Effect of NaCl on growth

For the NaCl tolerance experiment, 200 µL of a culture with an optical density (OD) of 0.1 were inoculated into 5 mL of Horikoshi broth with varying NaCl concentrations ranging from 0 to 3 M (Ibrahim et al., 2019; Joshi et al., 2021). After 24 h of incubation at 37 °C with agitation at 150 rpm, optical density at 600 nm was measured using a UV-Visible spectrophotometer.

2.8. RAST tool for comparative genome analysis

From 16 S rRNA sequencing findings, the National Center for Biotechnology Information (NCBI) database was screened for whole genome sequences of identified isolates and obtained the sequences for the following bacterial species: 1) *Evansella cellullosilytica* DSM 2522, 2) *Alkalihalobacillus okhensis* Kh10-101, 3) *Halalkalibacterium halodurans* C-125, 4) *Sutcliffiella cohnii* DSM, 5) *Salpaludibacillus agaradhaerens* DSM 8721, and 6) *Alkalibacterium pelagium* DSM 19183. To analyze the genomic potential unique to each bacterial isolate further, the online RAST tool (<https://rast.nmpdr.org/rast.cgi>) was utilized (Joshi et al., 2021; Liu et al., 2022). The comparative table was then compiled, providing information about these organisms' genomes, metal tolerance traits, transporter protein genes, siderophores and hydrolytic enzymes.

2.9. Metal Tolerance

Based on the information obtained in the comparative genome analysis of metal tolerance traits, the most promising isolates (RPD 2.1, RPD 1.1, RPS 2.3, RPSS 1.1, RPCO 1, and RPCO 2) were selected for evaluating their metal tolerance. Six different metals, aluminum chloride (AlCl₃), potassium dichromate (K₂Cr₂O₇), cobalt nitrate (Co (NO₃)₂), mercury sulfate (HgSO₄), sodium tellurite (Na₂TeO₃), and copper sulfate(CuSO₄) were tested at concentrations ranging from 100 to 2000 ppm (except for sodium tellurite, which ranged from 100 to 1000 ppm, and mercury sulfate, which ranged from 50 to 1000 ppm). The metal stock solutions were added to sterile Horikoshi Broth, and cultures were adjusted to a density of 0.2 OD at 600 nm. Inoculation volumes of 200 µL were introduced into 20 mL of Horikoshi broth, followed by incubation at 37 °C with agitation at 150 rpm. The growth of the culture was measured spectrophotometrically at 600 nm, and based on the optical density (O.D), the tolerance index assigned to each isolate as follows: Tolerance index of 0.5 (O.D-0.1 to 0.5), 1 (O.D- 0.6 to 1.5), 2 (O.D-1.6 to 3) and 0.05 (if O.D is same as uninoculated control media).

2.10. Effect of red mud tolerance and pH modulation capacity

In the red mud tolerance experiment, solutions with red mud concentrations of 1%, 5%, and 10% were prepared by mixing sterile Horikoshi broth (excluding Na₂CO₃). To each solution, 1 mL of a culture with an optical density (OD) of 0.5 was added. The cultures were then incubated at 37 °C with agitation at 150 rpm for 7 days. Samples were collected at regular intervals for pH measurement and bacterial count. High-performance liquid chromatography was performed to detect organic acids in the samples.

2.11. High-performance liquid chromatography

Organic acid detection was done using HPLC Agilent 1260 system equipped with Hamilton PRPX 300 (150 × 4.1 mm, 7 µ) column. The sulphuric acid (0.5 mM) as a mobile phase 0.5 mL/min flow rate and 10 µL of injection volume (Pedram et al., 2020). The standard organic acids, namely ascorbic, oxalic, citric, lactic, tartaric, acetic and malic acids, were run at 100 ppm for identification. The detection was done using a UV-visible detector at 210 nm wavelength.

The isolated bacterial species were identified using 16 S-rRNA gene sequencing. The 16 S-rRNA gene sequences of 13 bacteria were

deposited to GenBank. The identified species and their assigned accession number have been given in Table S3.

3. Results

3.1. Red mud characterization

Red mud's characteristics are primarily defined by its pH and elemental composition. Literature indicates its pH varies from 10 to 13, depending on the location, age and type of Bauxite mineral used (Evans 2016; Mud et al., 2019; Power et al., 2011). Likewise, for the collected sample, the pH of fresh red mud was in the range of 10–11 (Table S1, supplementary information). X-ray fluorescence (XRF) revealed the major phases as aluminum oxide, iron oxide, silica oxide, sodium and titanium oxide (Table 2). Inductively coupled plasma optical emission spectroscopy (ICP-OES) confirmed these major elements and identified additional minor elements, including precious metals (Sc, V, Se and Cu) and heavy metals (Cd, Co, As, Pb, Cr and Zn). Further, infrared spectroscopy identified prominent absorption bands at 3451.96, 2856.06, 2925.48, 1641.13, 1427.07, 1357.64, 997.02, 800.31, 570.82, and 451.26 cm⁻¹ (Fig. S1). The peak at 3451.96 cm⁻¹ indicates hydroxyl bonds in silicates, goethite and gibbsite (Konadu et al., 2013; Muci et al., 2021). The peak at 1641.13 represents free H₂O in the mineral. The doublet at 1427.07–1357.64 cm⁻¹ signifies asymmetric C–O bond stretching, suggesting the presence of carbonate in calcite (Singh et al., 2019). The peaks at 997 cm⁻¹ and, 570.82 and 451.261 cm⁻¹ correspond to Si–O bond Fe–O bonds, respectively (La et al., 2008).

3.2. Enrichment and isolation of bacteria from red mud

A total of 15 pure colonies were isolated from seven different red mud samples divided into four layers (surface, subsurface, deep and carbonate). Each isolate was labelled for identification, such as RPS1.1 representing the first colony isolated from the RPS1 sample. These pure cultures were preserved on agar plates and in glycerol stocks at -80 °C. Detailed morphological characteristics are provided in Table S2 (supplementary information). 16 S-rRNA sequencing and phylogenetic analysis were performed to identify the bacterial genera. Table S3 summarizes all isolate identifications and key characteristics. Notably, isolates RPS1.1, RPSS1.1, and RPSS2.1 demonstrated similar 16 S-rRNA sequences, suggesting a shared species identity. Therefore, for subsequent analyses, only the isolate RPSS1.1 was chosen for further studies.

As previously mentioned, red mud samples were collected from different depths to capture both air-borne bacterial species (surface and subsurface) and red mud-adapted (deep and carbonate layers). Surface and subsurface samples were predominantly populated by alkaliphilic *Bacillus* species, while unique species adapted to hypersaline environments, like *S. agaradhaerens*, *A. okhensis*, *E. cellullosilytica*, and *Nesterkonia* sp., were found in the carbonate layer and deep layer samples. Multiple studies have reported the presence of these specific species in soda lakes and salt pans. For example, *E. halocellulosilyatica* has been isolated by Liu et al. (2022) from red mud collected from Chiping County, China. Similarly, *A. okhensis* sp. has been isolated from Indian

salt pan (Nowlan et al., 2006). A very recent study showed *A. okhensis* strain Kh10-101 T produced highly alkaline stable subtilisins (Falkenberg et al., 2022). Alkaline serine-protease-producing strain of *S. agaradhaerens* AK-R, formerly known as *B. agaradhaerens*, was isolated from an Egyptian soda lake (Ibrahim et al., 2019). The same research group also reported reduction of chromium using *S. agaradhaerens* strain NRC-R (Ibrahim et al., 2022).

3.3. Construction of phylogenetic tree

A phylogenetic tree (Fig. 1) was constructed using MegaX software, revealing the genetic relationships among these isolates and their placement within the broader context of bacterial taxonomy. This analysis was carried out in accordance with the previously described methodology, which included 16 S-rRNA sequencing, PCR protocols, and primer sequences.

3.4. Growth curve

The major limitation for employing bacterial cultures in large scale bioremediation process is their slower growth kinetics (Cozzolino et al., 2023). Hence, it is very crucial to determine the growth rates of isolates in order to select it for further treatments. In the present study most of the isolates exhibited growth at a pH of 10.3 ± 0.2 with a lag period lasting between 4 and 8 h. However, RPS 1.2 was outlier. As it didn't grow in standard Horikoshi broth during the 72 h observation period. However, addition of NaCl to Horikoshi broth triggered growth after 24 h, indicating a dependency on sodium for growth. In contrast, RPSS2.2 was faster growing, reaching the stationary phase earlier in comparison to the other isolates. (Refer to Figure S2 a: Growth Curve.).

3.5. Effect of pH on the growth

Red mud bioremediation perquisite the alkaline tolerance in the selected microbial species (Santini et al., 2016). Therefore, the isolates were subjected to grow in presence of different pH (Gao et al., 2024). As depicted in Fig. S3a, it is evident that all the tested isolates exhibited growth starting from a pH of 8, except for RPCO4, RPS2.3, and RPSS2.2, which initiated growth at a pH of 7. The optimal pH range for most isolates fell within 10–10.5, with the exception of RPS1.2, which displayed its best growth at pH 9. In accordance with Horikoshi's definition of alkaliphiles, it can be inferred that, apart from RPCO4, RPS2.3, and RPSS2.2, the remaining isolates can be categorized as alkaliphiles (Horikoshi 1999). Out of 13 isolates, nearly 7 isolates (RPS2.2, RPS2.2, RPS2.3, RPCO1, RPCO4, RPSS2.2, RPSS2.3, RPD1.1, RPD1.2) showed 2.5–3-unit reduction at 10–10.5 pH range. The affinity for high pH associated with the pH drop which is remarkably higher than the previous findings (Dey and Paul 2021; Feigl et al., 2024). Further analysis revealed that most isolates, showed minimal reduction in the pH of the medium when they grow at 8–9 pH range. Thereafter sharp decrease in medium's pH as growth maximizes above 9 pH suggesting at higher pH there is an imperative need to lower the medium's pH. Likewise, RPSS2.2, exhibiting consistent optical density from pH 7–10 (optimal at 7), demonstrates increased reduction at pH 10, implying a heightened pH triggers mechanisms, such as organic acid production, for pH reduction. Paavilainen et al., proposed that alkaliphiles favor low molecular weight acids like acetic acid in high pH environments (Paavilainen et al., 1994; Wilks et al., 2009). Similarly, Wilks et al. (2009), suggested that at high pH, genes for catabolism of carbon and production of organic acid are upregulated in alkali-tolerant *Bacillus subtilis*. This showcase that the higher pH triggers excretion of acidic metabolites by bacteria in the medium (Wilks et al., 2009).

3.6. Effect of NaCl on growth

Red mud found to be a hypersaline environment thus, halophilic

Table 2
Elemental analysis of red mud using XRF and ICP-OES study.

Metal	XRF		ICP-OES		
	Concentration (wt. %)	Metal	Concentration mg/Kg*10 ²	Metal	Concentration mg/Kg*10 ²
Al ₂ O ₃	19.3	V	0.13	Cd	0.29
Fe ₂ O ₃	49.27	Sc	13.8	Co	0.17
CaO	1.74	Mg	74.7	Cr	3.82
Na ₂ O	5.98	Mn	4.44	Cu	0.6
P ₂ O ₅	0.09	Zn	43.4		
SiO ₂	7.00	Pb	0.06		
TiO ₂	3.94	As	3.5		

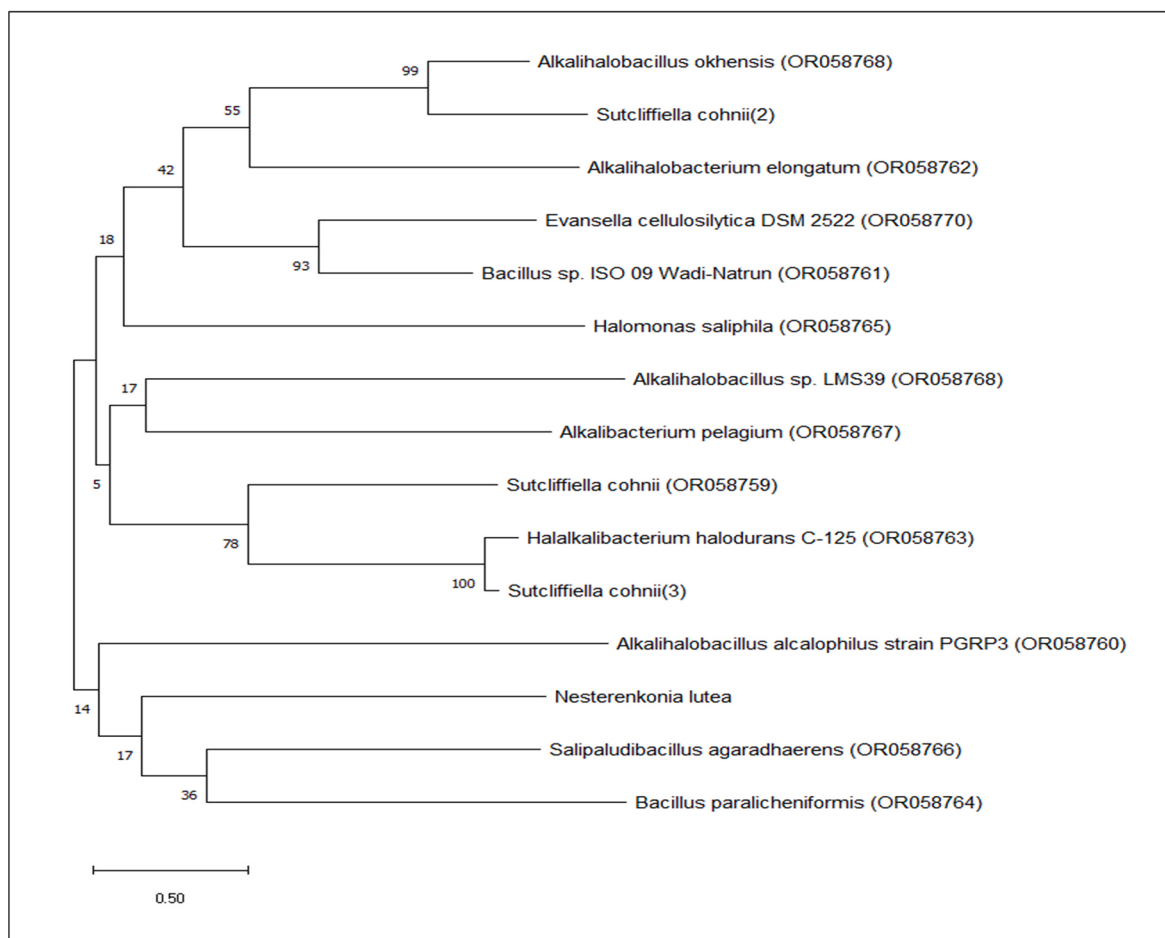


Fig. 1. Phylogenetic tree of 15 bacterial isolates from red mud. (Phylogenetic tree is constructed using MegaX software highlighting the relationship among 16 S rDNA gene sequences from red mud samples. The trees were constructed using the neighbour-joining tree. The values indicate the percentage of occurrence in 1000 bootstrapped trees and the scale bar represents 0.5 nucleotide substitution.

microbial species may seem to be survive in it (Santini et al., 2015). Similar observations from Fig. S2b, reveal that all tested isolates exhibited growth within the NaCl concentration range of 0–2 M, while none of the isolates were able to grow at 3 M NaCl. Notably, there was a significant decline in growth for all isolates starting from 1 M NaCl, suggesting that the optimal concentration falls within the range of 1–1.5 M, except for RPSS1.1, which exhibited optimum growth at 2 M NaCl. Therefore, these isolates can be categorized as moderate halophiles. However, it's important to note that RPSS2.2, RPSS2.3, RPS2.1, RPS2.3, RPD1.1, and RPS1.2 did not demonstrate any growth at 2 M NaCl. On the other hand, RPCO1, RPCO2, and RPCO4 displayed robust growth within the 0.5–2 M NaCl range, which can be attributed to their adaptation to the carbonate layer of the red mud pond from which they were isolated. Furthermore, it's worth mentioning that RPSS1.1, RPS2.1, and RPD1.2, identified as *S. cohnii*, *Bacillus* sp., and *E. cellullosilytica*, respectively, also exhibited a higher tolerance to NaCl. RPS1.2 exhibited peak growth at a concentration of 0.5 M NaCl, and its sluggish growth in Horikoshi medium (pH 10.3) suggests the significance of NaCl for optimal growth (Fig. S3b). This suggests a potential connection between their environmental origin and their ability to thrive in saline conditions.

3.7. Genome comparison and functional annotation of red mud isolates

This study employed RAST server for genome comparison of six closely related bacterial reference strains with isolates identified from red mud samples: 1) *E. cellullosilytica* DSM 2522, 2) *A. okhensis* Kh10-101,

3) *H. halodurans* C-125, 4) *S. cohnii* DSM6307, 5) *S. agaradhaerens* DSM 8721, and 6) *A. pelagium* DSM 19183. These bacterial species were matching closely to the 6 identified isolates RPD1.2, RPD1.1, RPS2.3, RPSS1.1, RPCO1, and RPCO2 respectively. Table S4, summarizes their overall genome size, GC content and coding region. The metal tolerance genes present in these bacteria were examined using RAST, which identifies domains associated with resistance to aluminum, copper, cadmium, cobalt, mercury and tellurite resistance domains. These findings were subsequently validated experimentally and are discussed in the following section. The results obtained in metal tolerance experiment (Fig. 2) were further correlated with the metal tolerance genes identified in these bacteria (Table S5). The efflux pump/transporter proteins play crucial role in metal tolerance their distribution in the isolates has been depicted in Fig. S4. The RAST analysis also revealed the potential of these exopolysaccharide and hydrolytic enzymes, which are important for metal mobilization and bioremediation processes. In our preliminary analysis (data not shown here) all 13 isolates were screened for exopolysaccharide production using ethanol precipitation method. Among them, five isolates, namely, RPS2.3, RPSS2.3, RPCO4, RPD1.1 and RPD1.2 demonstrated exopolysaccharide production. The presence of the Anthrachelin siderophore gene was detected in four of the reference bacteria in RAST analysis: *E. cellullosilytica* DSM 2522, *H. halodurans* C-125, *S. cohnii* DSM6307, *S. agaradhaerens* DSM 8721 (Table 3). Siderophores, which are primary metal-chelating agents, can significantly enhance the suitability of these isolates for metal extraction process (Emmanuel et al., 2012; Gascoyne et al., 1991).

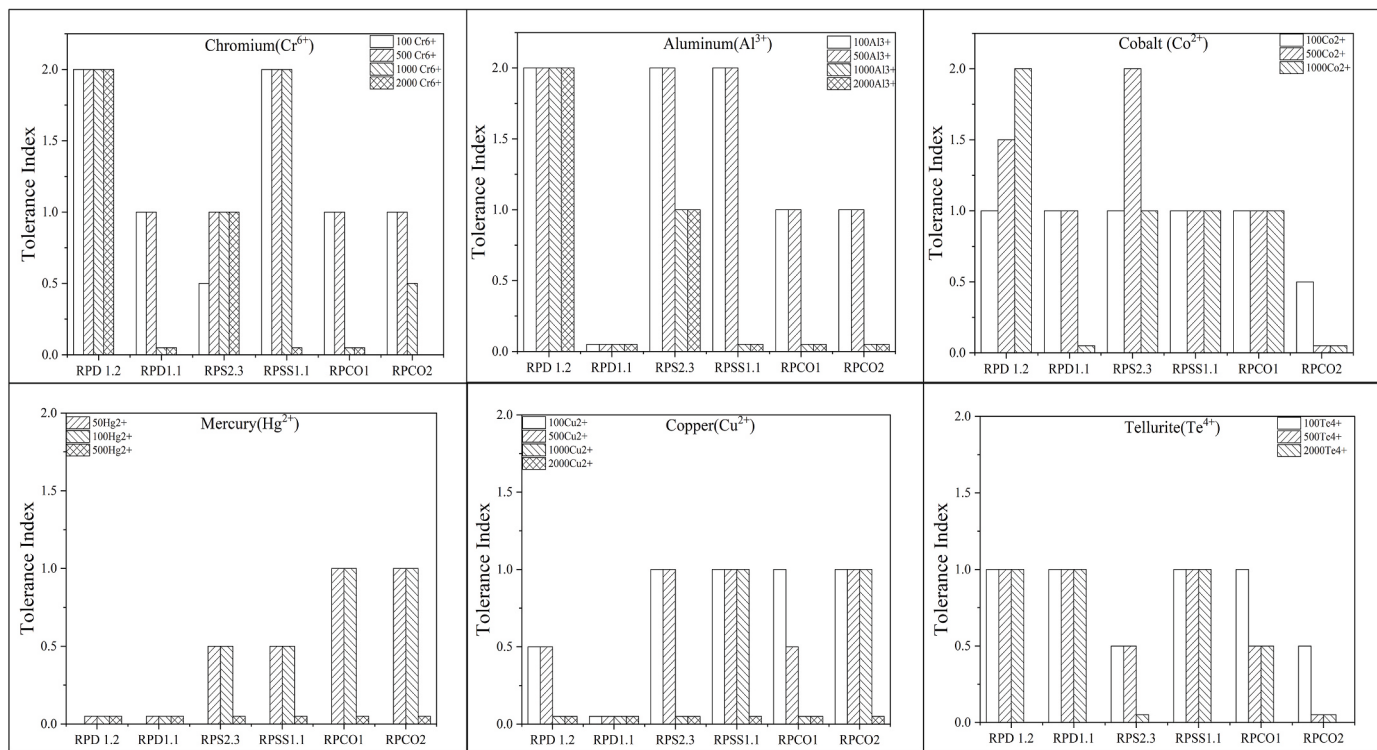


Fig. 2. Metal tolerance study: Experimental findings of tolerance pattern of chromium, tellurite, aluminum, copper, cobalt and mercury in RPCO1, RPCO2, RPD1.1, RPD1.2, RPS2.3 and RPSS1.1 respectively.

Table 3

Siderophore, hydrolytic enzymes and EPS production genes found in bacterial isolates using RAST tool.

Genes/isolates	<i>Evansella cellulosilytica</i> DSM 2522	<i>Alkalihalobacillus okhensis</i> Kh10-101	<i>Halalkalibacterium halodurans</i> C-125	<i>Sutcliffiella cohnii</i> DSM 6307	<i>Salipaludibacillus agaradhaerens</i> DSM 8721	<i>Alkalibacterium pelagium</i> DSM 19183
Siderophore Enzymes	Anthrachelin Xylanase & cellulase	NA NA	Anthrachelin Xylanase	Anthrachelin NA	Anthrachelin Xylanase & cellulase	NA Xylanase
Exopolysaccharide Production	NA	Present	Present	Present	NA	Present

Key: NA- Information is not available.

3.8. Metal tolerance study has been discussed one by one in following section

3.8.1. Aluminum tolerance

All tested strains exhibited varying degrees of tolerance to aluminum chloride (AlCl_3), with RPD1.2 and RPS2.3 demonstrating the highest tolerance, enduring up to 2000 ppm. In fact, RPS1.2 showed highest tolerance index at all tested concentration of AlCl_3 . RPSS1.1, RPCO1, and RPCO2 showed intermediate tolerance levels up to 1000 ppm. Notably, RPD1.1 displayed the lowest aluminum tolerance, with a limit of 100 ppm (Fig. 2). RAST analysis revealed the presence of aluminum-resistant protein genes in all isolates, except for RPCO2, implying additional mechanisms contributing to aluminum tolerance (refer to Table S5). These isolates were sourced from environments rich in aluminum, potentially contributing to their increased tolerance. The presence of aluminum-tolerant endophytic fungi and bacteria can promote plant growth in acidic soil (Barra et al., 2023; Hazarika et al., 2023). Although information on the molecular mechanisms underlying aluminum tolerance in bacteria is limited, several studies link it to acid production and siderophore synthesis (Hazarika et al., 2023). Recent study by Barra et al. (2023) shown that the production of citrate and malate plays a role in aluminum chelation. The presence of siderophore

synthesis genes in RPCO1, RPSS1.1, RPS2.3, RPD1.1, and RPD1.2, as revealed by RAST analysis, aligns with this potential mechanism. Moreover, these isolates are capable of reducing the medium pH by 2–3 units, suggesting that aluminum tolerance may be associated with acid and siderophore synthesis, as reported in the literature.

3.8.2. Tellurite tolerance

All isolates were found to possess tellurite-resistant protein genes according to RAST analysis, with the exception of RPCO2 as given in Table S5. Experimental results aligned with these findings. RPD1.2, RPD1.1, RPSS1.1, and RPCO1 were capable of reducing 1000 ppm of sodium tellurite (Na_2TeO_3), while RPS2.3 exhibited reductions up to 500 ppm (Fig. 2). This reduction of tellurite (Te^{4+}) to tellurium (Te^0) was visually confirmed by medium blackening. RPCO2 displayed a limited tolerance of 100 ppm and lacked reduction capabilities. Tellurite reduction in bacteria is often associated with the presence of intracellular free thiol groups, which are commonly found on enzymes facilitating tellurite reduction (Muñoz-Díaz et al., 2022). Some bacteria even use tellurite (Te^{4+}) as a terminal electron acceptor, leading to its accumulation on the cell surface as a black precipitate of tellurium (Te^0). Intracellular accumulation of tellurium nanoparticles has also been observed in bacteria, representing an enzymatic process (Ollivier et al.,

2008).

3.8.3. Chromium tolerance

The tested isolates exhibited varying degrees of tolerance to potassium dichromate ($K_2Cr_2O_7$), with RPD1.2 and RPS2.3, withstanding highest at 2000 ppm, followed by RPSS1.1 and RPCO2, capable of tolerating 1000 ppm. However, though RPS2.3 could tolerate 2000 ppm concentration its growth in terms of tolerance index were lesser compared to RPD1.2. The RPD1.1 and RPCO1 exhibited lower tolerance, with limits of approximately 500 ppm. RAST analysis (Table S5, Fig. S4) revealed the presence of chromium reductase and transporters genes in all six species. Various studies have reported the role of chromate reductase in the detoxification of chromium in bacteria and fungi (Mary Mangaiyarkarasi et al., 2011; Viti et al., 2014). Chromate reductase converts Cr^{6+} to Cr^{3+} , which is then detoxified by other molecular mechanisms. Chromate reductases are NADH:Flavin oxidoreductases with broad substrate specificity. Another mechanism of tolerance found in bacteria is efflux pumps that expel chromium ions from the cell cytoplasm (Viti et al., 2014). In haloalkaline environments like those favored by current isolates, the dominant chromium form at high pH is CrO_4^{2-} . As the pH drops due to bacterial growth, it shifts towards the more mobile $HCrO_4^-$. This form readily binds to hydroxyl, carbonyl, and phosphate groups on the biomass and can be transported across the cell membrane for subsequent reduction by chromate reductase (Karthik et al., 2017; Vendruscolo et al., 2017). The production of organic acids by organisms is crucial during the initial stages of metal tolerance. Sporulation has been seen to increase the threshold concentration of chromium toxicity in *Bacillus* sp. (Viti et al., 2014). Recently, Ibrahim et al. (2022) isolated *S. agaradhaerens* strain NRC-R from a hypersaline soda lake, capable of reducing chromium around 888.5 ppm in 16 h and 1177 ppm in 32 h. In this study, RPCO1 has been identified as *S. agaradhaerens* (99.92% similarity), which could tolerate 500 ppm and showed no growth at 1000 ppm.

3.8.4. Mercury tolerance

RAST analysis identified two major mercury resistance proteins, including the mercuric resistance operon regulatory protein and MerR mercuric ion reductase, in RPD1.1, RPD1.2, and RPCO2. However, experimental data did not conclusively correlate these proteins with mercury sulfate ($HgSO_4$) tolerance. RPD1.1 and RPD1.2 proved sensitive to even 50 ppm mercury (Hg^{+2}), while RPSS1.1 tolerated only 50 ppm. RPS2.3, RPCO1, and RPCO2 exhibited tolerance up to 100 ppm. This apparent disconnect between genetic potential and phenotypic expression warrants further investigation.

3.8.5. Copper tolerance

All isolates, with the exception of RPD1.1, demonstrated a degree of tolerance to copper sulfate ($CuSO_4$). Specifically, RPD1.2, RPS2.3, and RPCO1 exhibited tolerance to 500 ppm, while RPSS1.1 and RPCO2 displayed resilience to 1000 ppm. RAST analysis identified several copper resistance-related proteins, including copper resistance protein, copper homeostasis protein, and copper-translocating P-type ATPase (Ge et al., 2021; Ladomersky and Michael, 2015; von Rozycki et al., 2009). However, the presence of these genes did not always correlate with tolerance. Despite RPCO2 having the highest number of copper-translocating P-type ATPase genes (12), it did not exhibit higher tolerance compared to other isolates. Conversely, RPD1.1, with one copper resistance protein and one copper-translocating P-type ATPase gene, showed no copper tolerance, indicating multiple mechanisms of resistance. Clausen et al. (2000) highlighted the significance of oxalic acid in copper tolerance. As elaborated in section 3.9, the halo-alkaliphilic strains isolated in this study demonstrate the ability to produce mixed organic acids, suggesting a potential association with copper tolerance in RPD1.1.

3.8.6. Cobalt tolerance

RAST analysis revealed the presence of Cobalt-zinc-cadmium resistance protein genes in all isolates. Experimental data confirmed RPD1.2, RPS2.3, RPSS1.1, and RPCO1's ability to tolerate 1000 ppm of cobalt nitrate ($Co(NO_3)_2$), while RPD1.1 exhibited tolerance up to 500 ppm, and RPCO2 showed the lowest tolerance, up to 100 ppm. Different Cobalt/zinc/cadmium resistance protein genes like CzcA and CzcD were found to be present in the isolates. Moreover, a transcriptional regulator-MerR family, which functions as a cobalt-zinc-cadmium resistance protein, was also present in all the screened isolates. The czc cobalt-zinc-cadmium resistance determinant found to confer tolerance to many metals, including cobalt, in *C. metallidurans*, which is a model organism for metal detoxification (Nies, 1995; von Rozycki et al., 2009). However, the low tolerance of RPCO2, despite having the highest number of cobalt-zinc-cadmium resistance protein genes, was not conclusive. RAST analysis of efflux pumps/transporters indicated that RPCO2 had the minimum number of efflux/transporter genes, which might contribute to its lower tolerance to copper and cobalt (Fig. S4).

Based on tolerance index data, the RPD1.2 isolate identified as *E. cellullosilytica* exhibited robust growth in the presence of Al^{3+} , Cr^{6+} and Co^{2+} followed by RPS2.3 (*H. halodurans*) and RPSS1.1 (*S. cohnii*). Conversely, all isolates showed lower tolerance for Te^{4+} , Cu^{2+} , Hg^{2+} metals, possibly due to their prevalence in the red mud source from which they are isolated. This study also highlighted the remarkable multi-metal tolerance of these haloalkaliphiles, driven by a complex interplay of genetic predisposition and potentially unique adaptation strategies. Even isolates lacking specific metal resistance genes are capable of tolerating that particular metal, likely due to constant exposure to diverse metal environments and potential cross-resistance or alternative ion export mechanisms.

3.9. Mechanism of multi-metal tolerance

The probable mechanism of multi-metal tolerance in these haloalkaliphiles was elucidated based on the experimental findings and RAST analysis of transporter proteins, metal reduction proteins, organic acid production and presence of siderophores (Fig. 3). Metals and metalloids can enter the bacterial cell through various modes. One mode is adsorption onto the extracellular polymeric matrix (Hussein et al., 2019). As previously mentioned in section 3.7, strains RPS2.3, RPSS2.3, RPCO4, RPD1.1, and RPD1.2 exhibited EPS production. Additionally, RAST analysis supports the presence of EPS production genes in RPSS1.1, RPD1.1, RPS2.3 and RPCO2, indicating that metal ion adsorption is feasible in these species when present in metal-rich environments. Another pathway involves iron-chelating ligands like siderophores, which can form bonds with other metals like Al^{3+} and facilitate their entry into the cell (Edberg et al., 2010; Emmanuel et al., 2012). RAST analysis showed that strains RPCO1, RPD2.1, RPS2.3, and RPSS1.1 have the potential to produce siderophores. Additionally, membrane proteins act as channels for metal ion entry (Barra et al., 2023). The transporter proteins mentioned in Table S5 and Fig. S4 confirm the presence of sufficient metal channels in the tested bacteria. Once inside the cell, metals must be modified into less toxic forms to alleviate toxicity. This is often achieved by proteins or organic biomolecules like acids. Organic acid production plays a crucial role in metal complexation, as it increases the solubility of metal ions by lowering the pH in metal-rich environments (Astuti et al., 2016; Mishra and Rao 2020). This is significant for extracting metals from red mud. Additionally, enzymatic reduction of metals such as Cr^{6+} , Te^{4+} , and Hg^{2+} is also possible due to the presence of respective reductase proteins in the isolates. Efflux pumps, which export metals outside the cell using energy generation, may provide cross/non-specific-tolerance to multiple metals.

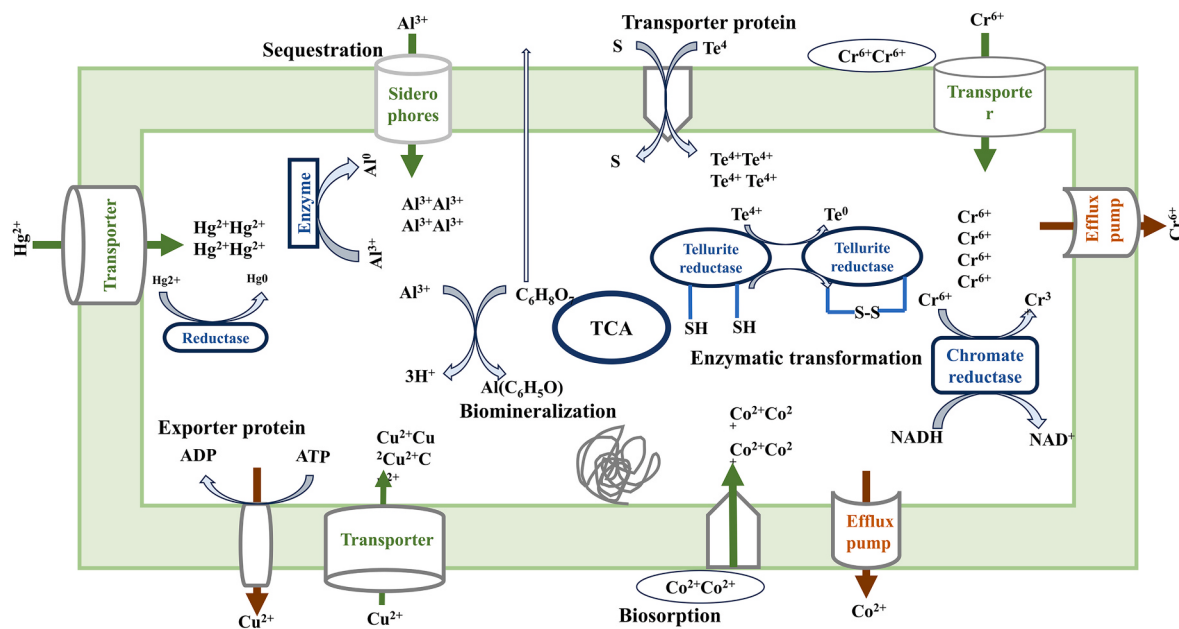


Fig. 3. Probable Mechanism of Metals Tolerance: Biosorption on EPS, sequestration through siderophores and transport through membrane proteins are some of the major mode of entries of metals inside the bacterial cell. The tolerance towards the metals and metalloids enhanced due biomineralization (production of organic acids for metal complexation), enzymatic modification (reduction and oxidation of metals changes its ionic form) and efflux pumps (exporting the metals outside the cell may or may not involve through energetic reactions).

3.10. Red mud tolerance and its pH modulation study

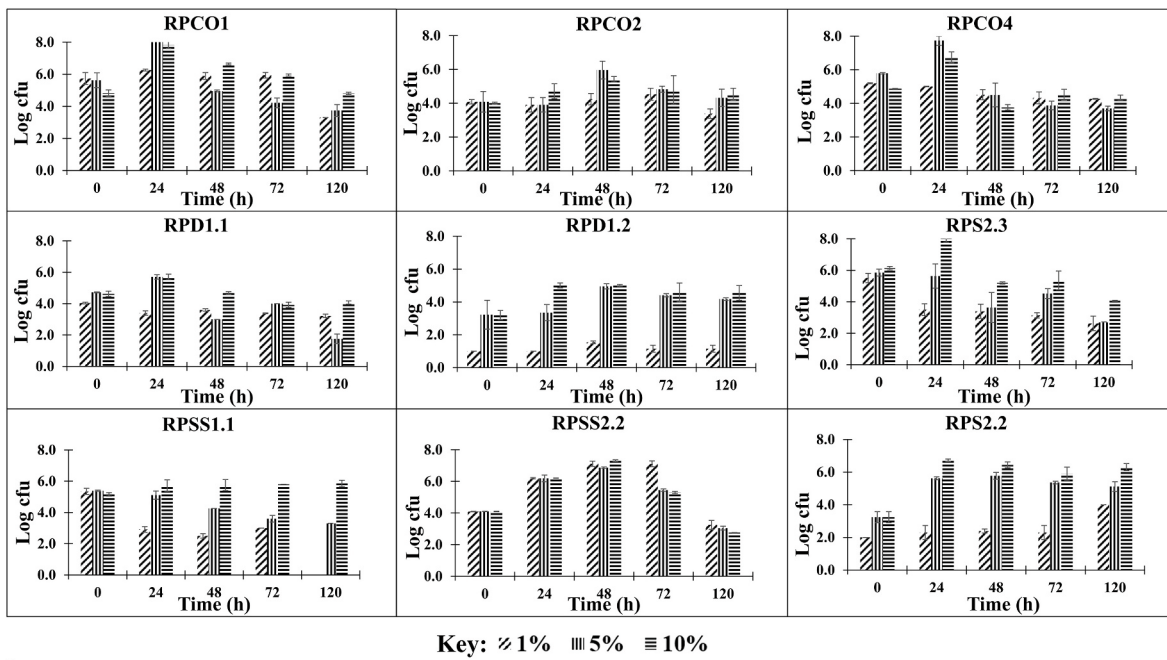
The alkali-halophilic strains isolated and identified in this study met all the inclusion criteria previously outlined for red mud bioremediation (Hamdy, 2001; Santini et al., 2015). Their tolerance to alkalinity, salinity and metal environments enhances their survival potential in the presence of red mud. Therefore, the tolerance and pH modulation capabilities of the 13 bacterial isolates were further examined in different concentrations of red mud supplemented with Horikoshi medium, excluding sodium carbonate. (Fig. 4a and 4 b). Red mud suspensions at 1%, 5%, and 10% exhibited initial pH values of 8, 8.8, and 9.3, respectively, due to the buffering effect of yeast extract in the medium. From, the results it can be interpreted that the tested isolates could tolerate 10% of red mud, demonstrating remarkable adaptability to the harsh alkaline environment. In accordance with pH optimization data, the cell growth was not significantly increase with 1% red mud as it has initial pH in the range of 7.8–8, except for RPSS2.2 which showed increase cell count at 1% as well. Therefore, the pH drop was also not significantly decreased in case of 1% red mud except for RPCO4, RPSS2.2, RPS2.3 and RPSS1.1. They could significantly reduce the pH to neutral range 6–7 from 8 at 1% red mud (1–2 units' reduction). Except for RPSS2.2, all isolate's, maximum growth occurred at 10% red mud, accompanied by a pH drop from 9.3 to 9.5 to 6–7 range (2.5–3.5 units' reduction) within 24 h of incubation. At 5% red mud, moderate growth and pH reductions (from 8.8 to 6.5–7) were observed in comparison to the 10% solution. For RPD1.2, though there was increase in cell count at both 5% and 10% red mud the pH reduction was strikingly different 0.8-unit reduction for 5% whereas 3 units for 10%. This indicates higher pH dependent activation of neutralization mechanisms. The RPD2.1, RPS1.2, RPSS2.3, and RPS2.1 did not show significant growth in the presence of red mud and thus no major reduction in pH of the red mud solution was observed till 5 days of incubation except for 0.5–1 unit of pH reduction at 10 % red mud concentration (Fig. S5, Supplementary information). These findings deviate from pH tolerance results and probably indicates metal toxicity from red mud. Previous studies reported non-indigenous fungal species have almost 10% red mud tolerance capacity but exhibiting the best metal leaching activity (based on organic acid production) at lower concentrations 1–2 % red mud within

10–15 days (Krishna et al., 2005; Qu et al., 2013, 2015). Red mud tolerant fungus *Trichoderma asperellum* RM-28 showed reduction in pH from 11 to 8.2 in 12 days of incubation (Anam et al. 2019). In contrast, current bacterial isolates displayed rapid and significant pH reduction at the highest red mud concentration (10%) within 24 h, suggesting their potential application for faster and more efficient red mud remediation strategies. Moreover, organic acid production has been associated with metal extraction from red mud in previous studies (Cozzolino et al., 2023; Kiskira et al., 2021; Qu and Bin, 2013). In all these studies, the production of mixed acids was favored by the bacterial/fungal strains. A similar detection of mixed acids was observed through HPLC analysis in the present study (Fig. S6). Based on their tolerance to red mud, RPCO1, RPCO4, RPSS1.1 and RPS2.3 exhibited the maximum reduction in pH at a 10% concentration. The supernatant from the red mud tolerance study was then analyzed for organic acid content, revealing that tartaric, acetic, and lactic acids were the primary agents for pH reduction, with a smaller amount of ascorbic acid present. In particular, RPSS1.1 exhibited the highest tartaric acid production at approximately 1876 ppm, while RPCO1 was the top lactic and acetic acid producer with 5316 ppm and 1787 ppm, respectively among all in presence of 10% red mud whereas. RPS2.3 also stood out as a significant lactic acid producer, generating 3884 ppm, while RPCO4 dominated in acetic acid production with 1670 ppm.

4. Discussion

Worldwide researchers are dedicating their efforts to reducing the growing volume of hazardous red mud. Sustainable pretreatment methods and bulk utilization are key gateways to achieve this goal. Recently, biobased methods for alleviating toxicity of red mud are a trending in the current research. While fungal cultures have been explored, their inherent flaws have shifted focus toward bacterial treatments. This study aimed to isolate and identify new multi-stress tolerant bacterial species, screen their genomic potential, and apply them in red mud bioremediation. To summarize, this study successfully isolated thirteen distinct haloalkaliphilic species from Indian red mud, showcasing their tolerance in high pH and salinity conditions, preference for pH 9–10 and tolerance up to 2 M NaCl. Experimental and RAST

a

Key: $\approx 1\%$ $\equiv 5\%$ $\equiv 10\%$

b

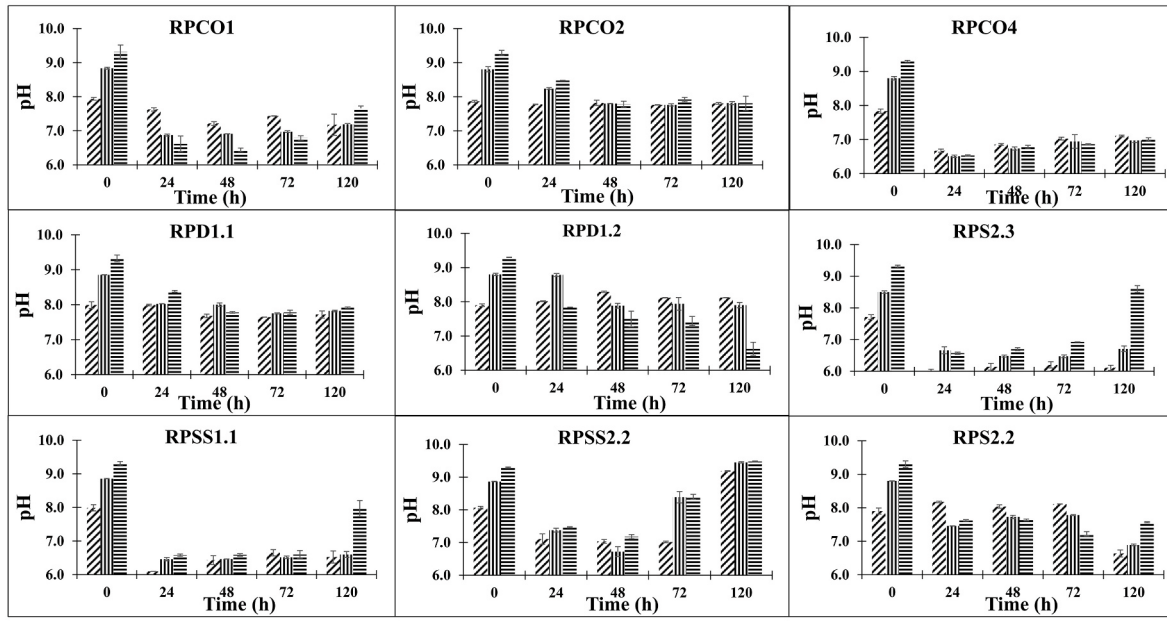
Key: $\approx 1\%$ $\equiv 5\%$ $\equiv 10\%$

Fig. 4. a) Red mud tolerance of the isolates (Growth of bacterial isolates was monitored in colony forming units against time in presence of 1%, 5% and 10% red mud concentrations). b) pH modulation capabilities of bacterial isolates grown in presence of 1%, 5% and 10% red mud concentrations.

findings revealed notable metal tolerance, particularly towards Al^{3+} , Cr^{6+} and Co^{2+} , exhibited by RPD1.2 (*E. cellulosilytica*), RPS2.3 (*H. halodurans*) and RPSS1.1 (*S. cohnii*) likely due to adaptation to the red mud environment. Particularly, RPD1.2 and RPS2.3 showed tolerance up to 2000 ppm of Al^{3+} and Cr^{6+} and 1000 ppm of Co^{2+} with high tolerance index. For RPSS1.1 the tolerance index was high at 1000 ppm of Cr^{6+} and Co^{2+} . Even though the individual tolerance to high pH, salinity and metals have been passed by these isolates it is not enough for their direct implementation in red mud bioremediation. Due to the complexity and inevitable toxicity of the red mud their survival in red mud has been checked. Among these isolates RPCO1, RPCO4, RPSS1.1

and RPS2.3 showed promising results for pH reduction capacity in the presence of 10% red mud, with pH levels decreasing from 9.3 to 9.5 to 6–7 within 24 h. This swift neutralization, facilitated by organic acid production, predominantly tartaric, acetic, and lactic acids, showcased promising results, surpassing those reported for non-indigenous strains (Ilkhani et al., 2024; Krishna et al., 2005). This notable pH decrease within 24 h is the quickest neutralization observed without the use of any external neutralizing agents, compared to previous research (Abhilash and Schippers, 2021; Zhang et al., 2022). Many reports suggest neutralization of red mud enables chances of vegetation on it (Rai et al., 2017). The sustainability of bio-based neutralization is

advantageous, as the increase in carbon, nitrogen, and associated minerals with microbial cultures leads to the succession of a microbiome that helps in the bulk utilization of red mud (Anam et al., 2019; Lv et al., 2022; Santini et al., 2016). Although, researchers have isolated microflora from red mud, but, their potential application in pH neutralization has not been extensively explored. One of the few studies involving Indigenous *Acetobacter* sp. showed its use in metal extraction from red mud. Currently, alkali-tolerant fungal and bacterial cultures are under investigation for red mud bioremediation (Anam et al., 2019; Lv et al., 2022). The major challenge lies in the tolerance capacity towards the red mud. Non-indigenous species cannot survive in red mud concentrations of 10% and above, limiting their scalability (Lv et al., 2022; Pedram et al., 2020; Qu et al., 2015). In this study, the indigenous species being haloalkaliphiles, are not only able to tolerate 10% of red mud but also neutralize it within 24 h. This rapid neutralization enhances the potential for direct utilization of red mud in various applications. Furthermore, using neutralized red mud for metal extraction can reduce the quantity and concentration of inorganic acids used in the process. RAST analysis suggests potential roles for siderophores and exopolysaccharides in metal biosorption, warranting further investigation. The biomolecules like EPS and siderophores extracted from the studied isolates can further aid in the separation of metals from the leaching medium. The combination of high metal tolerance observed in RPD1.2, RPS2.3, and RPSS1.1 along with acid production capacity of RPCO4, makes them as promising candidates for bio-assisted metal extraction. After evaluating survival rates in a multi-metal environment, pH regulation capacity of red mud, and the production of beneficial metabolites such as organic acids and EPS, it is clear that among the 13 haloalkaliphiles studied, RPS2.3 (*H. halodurans*), RPSS1.1 (*S. cohnii*), RPD1.2 (*E. cellulosilytica*), and RPCO4 (*Alkalihalobacillus* sp.) offer a sustainable and efficient approach for red mud dealkalization and metal recovery. Further exploring the metal extraction potential of these four isolates considering their strength of acid production in alkaline environment is needed from the perspective of the circular economy of Alumina industries.

5. Conclusion

This research successfully evaluated the potential of 13 isolated indigenous alkaliphilic species for red mud neutralization. These species thrive in pH 9–10 and tolerate up to 2 M NaCl. Experimental and RAST findings revealed notable metal tolerance, particularly towards Al^{3+} , Cr^{6+} and Co^{2+} , exhibited by RPD1.2 (*E. cellulosilytica*), RPS2.3 (*H. halodurans*) and RPSS1.1 (*S. cohnii*) likely due to adaptation to the red mud environment. Among these isolates RPCO1, RPCO4, RPSS1.1 and RPS2.3 showed promising results for survival and pH reduction capacity in the presence of 10% red mud. Remarkably pH levels decreased from 9.3 to 9.5 to 6–7 within 24 h achieving the fastest neutralization without any external neutralization agent. Overall, the four haloalkaliphilic strains RPS2.3 (*H. halodurans*), RPSS1.1 (*S. cohnii*), RPD1.2 (*E. cellulosilytica*), and RPCO4 (*Alkalihalobacillus* sp.) exhibit greater potential for utilization in red mud bioremediation efforts and in turn circular economy of Alumina industries.

Funding

This research did not receive any specific grant from funding agencies in the public, commercial, or not-for-profit sectors.

CRediT authorship contribution statement

Ankita Naykodi: Writing – original draft, Methodology, Investigation, Formal analysis, Data curation, Conceptualization. **Kruthi Doriya:** Writing – review & editing, Formal analysis. **Bhaskar N. Thorat:** Writing – review & editing, Supervision, Conceptualization.

Declaration of competing interest

The authors declare that they have no known competing financial interests or personal relationships that could have appeared to influence the work reported in this paper.

Data availability

Data will be made available on request.

Acknowledgments

The authors acknowledge the assistance from the National Aluminium Company Limited, Damanjodi plant, Odisha, India for acquiring red mud samples. Authors also appreciate Institute of Life Sciences, Bhubaneswar, Odisha, India for providing the research facilities.

Appendix A. Supplementary data

Supplementary data to this article can be found online at <https://doi.org/10.1016/j.ibiod.2024.105873>.

References

- Abhilash, Sabrina Hedrich, Schippers, Axel, 2021. Distribution of scandium in red mud and extraction using *gluconobacter oxydans*. *Hydrometallurgy* 202 (June 2020), 105621.
- Agnew, M. Dorothy, Koval, Susan F., Jarrell, Ken F., 1995. Isolation and characterization of novel alkaliphiles from bauxite-processing waste and description of *Bacillus Vedderi* Sp. Nov., a new obligate alkaliphile. *Syst. Appl. Microbiol.* 18 (2), 221–230.
- Anam, Giridhar Babu, Sudhakara Reddy, M., Ahn, Young Ho, 2019. Characterization of *Trichoderma asperellum* RM-28 for its sodic/saline-alkali tolerance and plant growth promoting activities to alleviate toxicity of red mud. *Sci. Total Environ.* 662, 462–469.
- Astuti, Widi, Hirajima, Tsuyoshi, Sasaki, Keiko, Okibe, Naoko, 2016. Comparison of effectiveness of citric acid and other acids in leaching of low-grade Indonesian saprolitic ores. *Miner. Eng.* 85, 1–16.
- Barra, Patrício Javier, Duran, Paola, Delgado, Mabel, Viscardi, Sharon, Claverol, Stéphane, Larama, Giovanni, Dumont, Marc, Mora, María de la Luz, 2023. Differential proteomic response to phosphorus deficiency and aluminum stress of three Al-tolerant phosphobacteria isolated from acidic soils. *iScience*, 107910.
- Clausen, C.A., Green, F., Woodward, B.M., Evans, J.W., 2000. Correlation between oxalic acid production and copper tolerance in *Wolfiporia Cocos*. *Int. Biodeterior. Biodegrad.* 46 (1), 69–76.
- Cozzolino, Anna, Cappai, Giovanna, Cara, Stefano, Milia, Stefano, Ardu, Riccardo, Tamburini, Elena, Carucci, Alessandra, 2023. Bioleaching of valuable elements from red mud: a study on the potential of non-enriched biomass. *Minerals* 13 (7).
- Dey, Satarupa, Paul, A.K., 2021. Evaluation of physio-biochemical potentials of alkaliphilic bacterial diversity in bauxite processing residues of diverse restoration history. *Environmental Sustainability* 4 (1), 155–169.
- Edberg, F., Kalinowski, B.E., Holmström, S.J.M., Holm, K., 2010. Mobilization of metals from uranium mine waste: the role of pyoverdines produced by *Pseudomonas fluorescens*. *Geobiology* 8 (4), 278–292.
- Emmanuel, E. S. Challara, Ananthi, T., Anandkumar, B., Maruthamuthu, S., 2012. Accumulation of rare earth elements by siderophore-forming arthrobacter luteolus isolated from rare earth environment of chavara, India. *J. Biosci.* 37 (1), 25–31.
- Evans, Ken, 2016. The history, challenges, and new developments in the management and use of bauxite residue. *Journal of Sustainable Metallurgy* 2 (4), 316–331.
- Falkenberg, Fabian, Rahba, Jade, Fischer, David, Bott, Michael, Bongaerts, Johannes, Siegert, Petra, 2022. Biochemical characterization of a novel oxidatively stable, halotolerant, and high-alkaline subtilisin from *Alkalihalobacillus okhensis* Kh10-101T. *FEBS Open Bio* 12 (10), 1729–1746.
- Feigl, Viktória, Medgyes-Horváth, Anna, Kari, András, Török, Ádám, Bombolya, Nelli, Berkli, Zsófia, Farkas, Éva, Fekete-Kertész, Ildikó, 2024. The potential of Hungarian bauxite residue isolates for biotechnological applications. *Biotechnology Reports* 41 (December 2023).
- Gadd, Geoffrey, M., Alan, J. Griffiths., 1977. Microorganisms and heavy metal Toxicity. *Microb. Ecol.* 4 (4), 303–317.
- Gao, Binyuan, Sun, Chongran, Yang, Tao, Cheng, Haina, Zhou, Hongbo, Wang, Yuguang, Zhu, Chen, 2024. Simultaneous dealkalization of red mud and recovery of valuable metals by a novel marine fungus tolerating high alkalinity and salinity. *J. Environ. Chem. Eng.* 12 (1), 111775.
- Gascoyne, D.J., Connor, J.A., Bull, A.T., 1991. Capacity of siderophore - producing alkaliphilic bacteria to accumulate iron, gallium and aluminum. *Appl. Microbiol. Biotechnol.* 36 (1), 136–141.

- Ge, Qing, Cobine, Paul A., Fuente, Leonardo De La, 2021. The influence of copper homeostasis genes copa and copb on xylella fastidiosa virulence is affected by sap copper concentration. *Phytopathology* 111 (9), 1520–1529.
- González Henao, Sarah, Ghneim-Herrera, Thaura, 2021. Heavy Metals in Soils and the Remediation Potential of Bacteria Associated With the Plant Microbiome. *Front. Environ. Sci.* 9 (April), 1–17.
- Gu, Ji-dong., 2016. Bioremediation of Toxic Metals and Metalloids for Cleaning Up from Soils and Sediments, pp. 2016–2019.
- Hamdy, M.K., 2001. Bacterial Amelioration of Bauxite Residue Waste of Industrial Alumina Plants. *J. Ind. Microbiol. Biotechnol.* 27 (4), 228–233.
- Hazarika, Dibya Jyoti, Sankar Bora, Sudipta, Singh Naorem, Romen, Sharma, Darshana, Boro, Robin Chandra, Barooah, Madhumita, 2023. Genomic insights into *Bacillus subtilis* MBB3B mediated Aluminium stress mitigation for enhanced rice growth. *Sci. Rep.* 1–16, 123456789.
- Horikoshi, Koki, 1999. Alkaliphiles: some applications of their products for Biotechnology. *Microbiol. Mol. Biol. Rev.* 63 (4), 735–750.
- Hussein, Mervat H., Hamouda, Ragaa A., Elhadary, Abdel Monsef A., Abuelmagd, Muhammad A., Ali, Shafaqat, Rizwan, Muhammad, 2019. Characterization and chromium biosorption potential of extruded polymeric substances from *synechococcus* mundulus induced by acute dose of gamma irradiation. *Environ. Sci. Pollut. Control Ser.* 26 (31), 31998–12.
- Ibrahim, Abdelnasser S.S., El-Tayeb, Mohamed A., Elbadawi, Yahya B., Al-Salamah, Ali A., 2011. Isolation and characterization of novel potent Cr(VI) reducing alkaliphilic *amphibacillus* Sp. KSUCR3 from hypersaline Soda Lakes. *Electron. J. Biotechnol.* 14 (4), 4.
- Ibrahim, Abdelnasser S.S., Elbadawi, Yahya B., El-Tayeb, Mohamed A., Al-maary, Khalid S., Maany, Dina Abdel Fattah, Ibrahim, Shebl Salah S., Elagib, Atif A., 2019. Alkaline serine protease from the new halotolerant alkaliphilic *Salipaludibacillus agaradhaerens* strain AK-R: purification and properties. *3 Biotech* 9 (11).
- Ibrahim, Mohamed, Abo, Alkaseem, Maany, Dina A., El, Mostafa A., Abdelnasser, Abd, 2022. Bioreduction of hexavalent chromium by a novel haloalkaliphilic *Salipaludibacillus agaradhaerens* strain NRC - R isolated from hypersaline soda lakes. *3 Biotech* 12 (1), 1–15.
- Ilkhani, Zahra, Vakilchian, Farzane, Sadeghi, Niloofar, Mousavi, Seyyed Mohammad, 2024. Base metals (Fe, Al, Ti) and rare earth elements (Ce, La, Pr) leaching from red mud through an efficient chemical-biological hybrid approach. *Miner. Eng.* 208 (August 2023), 108603.
- Joshi, Amaraja, Thite, Sonia, Karodi, Prachi, Joseph, Neetha, Lodha, Tushar, 2021. Alkalihalobacterium elongatum gen. Nov. sp. Nov.: an antibiotic-producing bacterium isolated from lonar lake and reclassification of the genus Alkalihalobacillus into seven novel Genera. *Front. Microbiol.* 12 (October), 1–22.
- Karthik, Chinnannan, Barathi, Selvaraj, Pugazhendhi, Arivalagan, Sri Ramkumar, Vijayan, Thi, Ngoc Bao Dung, Arulselvi, Padikasan Indra, 2017. Evaluation of Cr(VI) reduction mechanism and removal by *cellulosimicrobium funkei* strain AR8, a novel haloalkaliphilic bacterium. *J. Hazard Mater.* 333 (Vi), 42–53.
- Kiskira, Kyriaki, Theopisti Lymeropoulou, Lamprini Areti Tsakanika, Charalampos Pavlopoulos, Konstantina, Papadopoulou, Gerasimos Lyberatos, Maria, Ochsenkühn-Petropoulou, 2021. Study of Microbial Cultures for the Bioleaching of Scandium from Alumina Industry By-Products. *Metals* 11 (6), 1–11.
- Konadu, D.S., Annan, E., Buabeng, F.P., Yaya, A., 2013. Fabrication and characterisation of Ghanaian bauxite red mud-clay composite bricks for construction applications, 3 (5), 110–119.
- Krishna, Pankaj, Giridhar Babu, A., Sudhakara Reddy, M., 2014. Bacterial diversity of extremely alkaline bauxite residue site of alumina industrial plant using culturable bacteria and residue 16S rRNA gene clones. *Extremophiles* 18 (4), 665–676.
- Krishna, Pankaj, Sudhakara Reddy, M., Patnaik, S.K., 2005. *Aspergillus tubingensis* reduces the PH of the bauxite residue (red mud) amended soils. *Water Air Soil Pollut.* 167 (1–4), 201–209.
- Kulshreshtha, Niha Mohan, Kumar, Anil, Purnima, Dhall, Saurabh, Gupta, Bisht, Gopal, Pasha, Santosh, Singh, V.P., Kumar, Rita, 2010. Neutralization of alkaline industrial wastewaters using *exiguobacterium* Sp. Int. *Biodeterior. Biodegrad.* 64 (3), 191–196.
- La, A.O., Na, A.N.T.O., No, T.E.F.A., Zo, N., Ro, I.E.T., 2008. "XRD , FTIR , and thermal analysis of bauxite ore-processing waste (red mud) exchanged with heavy. *Metals* 56 (4), 461–469.
- Ladomersky, Erik, Michael, J. Petris, 2015. Copper tolerance and virulence in bacteria. *Metallooms* 7 (6), 957–964.
- Liu, Guo Hong, Rao, Manik Prabhu Narsing, Chen, Qian Qian, Che, Jian Mei, Shi, Huai, Liu, Bo, Wen, Jun Li, 2022. *Evansella halocellulosilytic* a sp. Nov., an alkalihalotolerant and cellulose-dissolving bacterium isolated from bauxite residue. *Extremophiles* 26 (2), 1–7.
- Lv, Kunyan Qiu, Shiji Ge, Zhiqiang Jiao, Chenyang Gao, Fu, Haiguang, Su, Rongkui, Liu, Zhongkai, Wang, Yulong, Yangyang, Wang, 2022. Neutralization and improvement of bauxite residue by saline-alkali tolerant bacteria. *Int. J. Environ. Res. Publ. Health* 19 (18).
- Mary Mangaiarkarasi, M.S., Vincent, S., Janarthanan, S., Subba Rao, T., Tata, B.V.R., 2011. Bioreduction of Cr(VI) by alkaliphilic *Bacillus subtilis* and interaction of the membrane groups. *Saudi J. Biol. Sci.* 18 (2), 157–167.
- Mishra, Manas Chandan, Rao, Bendadi Hanumantha, 2020. Neutralization of red mud with organic acids and assessment of their usefulness in abating PH rebound. *Journal of Hazardous, Toxic, and Radioactive Waste* 24 (1), 1–10.
- Musci, Gábor, Halyag, Nóra, Kurusta, Tamás, Kristály, Ferenc, 2021. Control of carbon dioxide sequestration by mechanical activation of red mud. *Waste and Biomass Valorization* 12 (12), 6481–6495.
- Mud, Red, Mutz, Dieter, Leader, Team, 2019. Rare Earths Extraction, pp. 9–10.
- Muñoz-Díaz, P., Jiménez, K., Luraschi, R., Cornejo, F., Figueroa, M., Vera, C., Rivas-Pardo, A., Sandoval, J.M., Vásquez, C., Arenas, F., 2022. Anaerobic RSH-dependent tellurite reduction contributes to *Escherichia coli* tolerance against tellurite. *Biol. Res.* 55 (1), 40659.
- Naykodi, Ankita, Patankar, Saurabh C., Thorat, Bhaskar N., 2023. Alkaliphiles for comprehensive utilization of Red Mud (Bauxite Residue)—an alkaline waste from the alumina refinery. *Environ. Sci. Pollut. Res.* 30 (4), 9350–9368.
- Nies, D.H., 1995. The cobalt, zinc, and cadmium efflux system CzcABC from *halcaligenes eutrophus* functions as a cation-proton antiporter in *Escherichia Coli*. *J. Bacteriol.* 177 (10), 2707–2712.
- Nogueira, Elis Watanabe, Hayash, Elize Ayumi, Alves, Enne, de Andrade Lima, Claudio Antônio, Adorno, Maria Talarico, Brucha, Gunther, 2017. Characterization of alkaliphilic bacteria isolated from bauxite residue in the Southern Region of Minas Gerais, Brazil. *Braz. Arch. Biol. Technol.* 60 (December), 1–7.
- Nowlan, Bianca, Dodia, Mital S., Singh, Satya P., Patel, B.K.C., 2006. *Bacillus okhensis* sp. Nov., a halotolerant and alkalitolerant bacterium from an Indian saltpan. *Int. J. Syst. Evol. Microbiol.* 56 (5), 1073–1077.
- Ollivier, Patrick R.L., Bahrou, Andrew S., Marcus, Sarah, Cox, Talisha, Church, Thomas M., Hanson, Thomas E., 2008. Volatilization and precipitation of tellurium by aerobic, tellurite-resistant marine microbes. *Appl. Environ. Microbiol.* 74 (23), 7163–7173.
- Paabila, Sari, Helistö, Pirkko, Korpela, Timo, 1994. Conversion of carbohydrates to organic acids by alkaliphilic bacilli. *J. Ferment. Bioeng.* 78 (3), 217–222.
- Panda, Ipsita, Surabhi Jain, Sarat Kumar Das, 2017. Characterization of red mud as a structural fill and embankment material using bioremediation. *Int. Biodeterior. Biodegrad.* 119, 368–376.
- Pedram, Hossein, Raouf Hosseini, Mohammad, Bahrami, Ataallah, 2020. Utilization of A. Niger strains isolated from pistachio husk and grape skin in the bioleaching of valuable elements from red mud. *Hydrometallurgy* 198 (March), 10549.
- Power, G., Gräfe, M., Klauber, C., 2011. Bauxite residue issues: I. Current management, disposal and storage practices. *Hydrometallurgy* 108 (1–2), 33–45.
- Qaidi, Shaker M.A., Tayeh, Bassam A., Isleem, Haytham F., de Azevedo, Afonso R.G., Ahmed, Hemm Unis, Emad, Wael, 2022. Sustainable utilization of red mud waste (bauxite residue) and slag for the production of geopolymers composites: A review. *Case Stud. Constr. Mater.* 16 (March), e00994.
- Qu, Yang, Bin, Lian, 2013. Bioleaching of rare earth and radioactive elements from red mud using penicillium tricolor RM-10. *Bioresour. Technol.* 136, 16–23.
- Qu, Yang, Li, Hui, Tian, Wenjie, Wang, Xiaoqing, Wang, Xuemeng, Jia, Xiaohui, Shi, Ben, Gendi Song, Yuan, Tang, 2015. Leaching of valuable metals from red mud via batch and continuous processes by using fungi. *Miner. Eng.* 81, 1–4.
- Qu, Yang, Li, Hui, Wang, Xiaoqing, Tian, Wenjie, Shi, Ben, Yao, Minjie, Ying, Zhang, 2019. Bioleaching of major, rare earth, and radioactive elements from red mud by using indigenous chemoheterotrophic bacterium *Acetobacter* Sp. *Minerals* 9 (2).
- Qu, Yang, Lian, Bin, Mo, Binbin, Liu, Congqiang, 2013. Bioleaching of heavy metals from red mud using *Aspergillus Niger*. *Hydrometallurgy* 136, 71–77.
- Rai, Suchita, Wasewar, K.L., Agnihotri, A., 2017. Treatment of alumina refinery waste (Red Mud) through neutralization techniques: A review. *Waste Manag. Res.* 35 (6), 563–580.
- Roh, Yul, Chul Min Chon, Ji Won, Moon, 2007. Metal reduction and biomining by an alkaliphilic metal-reducing bacterium, *alkaliphilus metallireducens* (QYMF). *Geosci. J.* 11 (4), 415–423.
- Santini, Talitha C., Kerr, Janice L., Warren, Lesley A., 2015. Microbially-driven strategies for bioremediation of bauxite residue. *J. Hazard Mater.* 293, 131–157.
- Santini, Talitha C., Malcolm, Laura I., Tyson, Gene W., Warren, Lesley A., 2016. PH and organic carbon dose rates control microbially driven bioremediation efficacy in alkaline bauxite residue. *Environ. Sci. Technol.* 50 (20), 11164–11173.
- Sarethy, Indira P., Saxena, Yashi, Kapoor, Aditi, Sharma, Manisha, Sharma, Sanjeev K., Gupta, Vandana, Gupta, Sanjay, 2011. Alkaliphilic bacteria: applications in industrial biotechnology. *J. Ind. Microbiol. Biotechnol.* 38 (7), 769–790.
- Shah, Syed Sikandar, Cesar Palmieri, Mauricio, Sponchiado, Sandra Regina Pombeiro, Bevilqua, Denise, 2022. A sustainable approach on biomining of low-grade bauxite by *p. simplicissimum* using molasses medium. *Braz. J. Microbiol.* 53 (2), 831–843.
- Singh, Smita, Aswath, M.U., Das, Rahul, V Ranganath, R., Choudhary, Harish K., Kumar, Rajeev, Sahoo, Balaram, 2019. Case studies in construction materials role of iron in the enhanced reactivity of pulverized red mud : analysis by Mössbauer spectroscopy and FTIR spectroscopy. *Case Stud. Constr. Mater.* 11, e00266.
- Tamura, Koichiro, Peterson, Daniel, Peterson, Nicholas, Stecher, Glen, Nei, Masatoshi, Kumar, Sudhir, 2011. MEGAS: molecular evolutionary genetics analysis using maximum likelihood, evolutionary distance, and maximum parsimony methods. *Mol. Biol. Evol.* 28 (10), 2731–2739.
- Tran, Lan-Huong, Tanong, Kulchaya, Jibir, A.D., Mercier, Guy, Blais, Jean-François, 2020. Hydrometallurgical process and economic evaluation alkaline batteries. *Metals* 10 (9), 1175.
- Vendruscolo, Francielo, Ferreira, Gláuber Luiz da Rocha, Filho, Nelson Roberto Antonisi, 2017. Biosorption of hexavalent chromium by microorganisms. *Int. Biodeterior. Biodegrad.* 119, 87–95.
- Viti, Carlo, Marchi, Emmanuela, Decorosi, Francesca, Giovannetti, Luciana, 2014. Molecular mechanisms of Cr(VI) resistance in bacteria and fungi. *FEMS (Fed. Eur. Microbiol. Soc.) Microbiol. Rev.* 38 (4), 633–659.
- von Rozicky, Torsten, Dietrich, H. Nies, 2009. Cupriavidus metallidurans: evolution of a metal-resistant bacterium. *Int. J. Gen. Molecul. Microbiol.* 96, 115–139, 2 SPEC. ISS.) Antonie.
- Ujaczki, Éva, Feigl, Viktória, Molnár, Mónika, Cusack, Patricia, Curtin, Teresa, Courtney, Ronan, O'Donoghue, Lisa, Davris, Panagiotis, Hugi, Christoph, Evangelou, Michael W.H., Balomenos, Eftymios, Lenz, Markus, 2018. Re-using

- bauxite residues: benefits beyond (Critical Raw) material recovery. *J. Chem. Technol. Biotechnol.* 93 (9), 2498–2510.
- Wilks, Jessica C., Kitko, Ryan D., Cleeton, Sarah H., Lee, Grace E., Ugwu, Chinagozi S., Jones, Brian D., Bondurant, Sandra S., Slonczewski, Joan L., 2009. Acid and base stress and transcriptomic responses in *Bacillus subtilis*. *Appl. Environ. Microbiol.* 75 (4), 981–990.
- Wu, Hao, Jia xin, Liao, Zhu, Feng, Millar, Graeme, Ronan Courtney, Sheng, guo Xue, 2019. Isolation of an acid producing bacillus Sp. EEELO2: potential for bauxite residue neutralization. *J. Cent. S. Univ.* 26 (2), 343–352.
- Zhang, Duo Rui, Chen, Hong Rui, Xia, Jin Lan, Nie, Zhen Yuan, Zhang, Rui Yong, Pakostova, Eva, 2022. Efficient dealkalization of red mud and recovery of valuable metals by a sulfur-oxidizing bacterium. *Front. Microbiol.* 13.
- Zhuang, Wei Qin, Fitts, Jeffrey P., Ajo-Franklin, Caroline M., Maes, Synthia, Alvarez-Cohen, Lisa, Hennebel, Tom, 2015. Recovery of critical metals using biometallurgy. *Curr. Opin. Biotechnol.* 33 (14), 327–335.